Available online at www.sciencedirect.com

ScienceDirect

Procedia Engineering 120 (2015) 167 – 170

Procedia Engineering

www.elsevier.com/locate/procedia

EUROSENSORS 2015

Biosensing at drop scale assisted by electrowetting at moderate frequency

Laurent Davoust[a], Johannes Theisen[a,b]

[a]*Grenoble Institute of Technology (Grenoble-INP) / Univ. Grenoble-Alpes / CNRS, SIMaP Laboratory, 1130 rue de la piscine, Dom. Universitaire, 38402 Saint Martin dHres, France*

[b]*CEA-Grenoble, LETI/DTBS, Minatec, 38000 Grenoble, France*

Abstract

This paper addresses surface ageing of a functionalized substrate in digital microfluidics. A model system based on bovine serum albumin (BSA)-laden sessile drop is selected. AC ElectroWetting-On-Dielectrics (EWOD), increasingly used in digital micro-systems for medical assays, is implemented in coplanar configuration. The small frequency required by EWOD actuation (f =100 - 1000 Hz) enables shape oscillations of the latter sessile drop and internal streaming. As demonstrated from dynamic contact angle (DCA) imaging, adsorption of BSA at the solid substrate is promoted under EWOD, as also shown from the time-dependent solid-liquid surface pressure. For an oscillating mode, n = 6, our numerical simulations show that corner eddies located near the oscillating contact line yield an efficient molecular renewal. In this way, oscillating EWOD could be used purposely as a tool to speed up label-free detection from DCA measurements.

Peer-review under responsibility of the organizing committee of EUROSENSORS 2015

Keywords: electrowetting, contact angle, digital microfluidics, biosensing, biofouling, biochip, EWOD

1. Introduction

Among most advanced techniques of digital microfluidics, ElectroWetting On Dielectrics (EWOD) [1] has become popular through the last years due to its abilities to generate and handle droplets by means of actuated electrode pairs buried under dielectric and hydrophobic layers. This paper is essentially relevant to biotechnological systems based on EWOD, particularly those devoted to biological environmental monitoring [2] or rapid on-board clinical diagnostics [3]. A proof-of-concept for label-free probing at drop scale is given in [4] where dynamic contact angle (DCA) measurements demonstrate that a solid phase assay based on DNA hybridization in a sessile drop drives a significant change in the solid-liquid surface tension. The present paper shows how coplanar EWOD in the oscillating regime (see electrode pair design in Fig. 1 of [7]) could reveal helpful for label-free biosensing based on such DCA measurements. Here, extensive use is made of BSA molecule since it is currently involved in heterogeneous reactions, for instance in the case of avidin adsorption on (BSA-coated) oxide surfaces of biochips [5]. The frequency of the EWOD actuation is also considered as a control parameter in the experiments.

Peer-review under responsibility of the organizing committee of EUROSENSORS 2015
doi:10.1016/j.proeng.2015.08.596

2. Materials and methods

A mother solution of BSA (extracted from bovine blood serum) at a concentration of 2 mg/mL was prepared from lyophilized powder of BSA at 98%. The solvent solution was prepared in reagent grade phosphate buffered saline (PBS, pH = 7.4). The final solution was adjusted to pH = 4 using hydrochloric acid (99% purity). The sessile drops involved in the experiments of this paper are characterized by a concentration of 30 μg/mL of BSA in a 100%PBS buffer at pH = 4 and room temperature (T=315K).

3. Supporting theory

DCA analysis is used here to investigate the kinetics of protein interaction with the surface of an EWOD chip. Using the measured dynamic contact angle, $\theta(U, C_0, t)$, and the applied voltage U, the surface tension γ_{SL} may be calculated from the Young-Laplace balance for a drop of volume concentration in BSA, C_0, and for a RMS voltage, U: $\gamma_{LG}\cos\theta\,(U, C_0, t) = \gamma_{SG} - \gamma_{SL}\,(U, C_0, t)$. Since we are only concerned with chemical transport within the drop, γ_{SG} is consistently supposed not to be affected by surfactant adsorption. The Young-Laplace balance can be written according to its usual form in non-contaminated conditions (100% PBS drop), $\gamma_{LG_0}\cos\theta_0 = \gamma_{SG} - \gamma_{SL_0}$, as well as in presence of BSA molecules, $\gamma_{LG}\cos\theta(0, C_0, t) = \gamma_{SG} - \gamma_{SL}\,(0, C_0, t)$. The symbols γ_{SL_0} and θ_0 are referred to as the solid-surface tension and the contact angle as obtained with no actuation and no BSA molecules (θ_0=$\theta(0, 0, t)$). As already mentioned, γ_{LG} (= 35mN/m) and γ_{SG} are considered as constant. The expression for the physicochemical surface pressure can be deduced from the latter balances:

$$\Pi_{SL} := \gamma_{LG}\cos\theta(0, C_0, t) - \gamma_{LG_0}\cos\theta_0, \tag{1}$$

Similarly, one also gets: $\gamma_{SL_0} - \gamma_{SL}\,(U, C_0, t) = \gamma_{LG}\cos\theta(U, C_0, t) - \gamma_{LG_0}\cos\theta_0$. Last, the dependence of γ_{SL} on U and the dependence of γ_{SL} on (C_o, t) can be dissociated by making use of the Lippmann equation for coplanar electrowetting, $\gamma_{SL}\,(U, C_0, t) = \gamma_{SL}\,(0, C_0, t) - \dfrac{c}{8}U^2$, where c, the capacity between the drop and the electrodes underneath, is defined from $c = (d_{\mathrm{Si_3N_4}}/\varepsilon_0\varepsilon_{\mathrm{Si_3N_4}} + d_{\mathrm{SiOC}}/\varepsilon_0\varepsilon_{\mathrm{SiOC}} + d_{\mathrm{oil}}/\varepsilon_0\varepsilon_{\mathrm{oil}})^{-1}$, with ε_0, the vacuum permittivity. The additional capacity contribution $d_{\mathrm{oil}}/\varepsilon_0\varepsilon_{\mathrm{oil}}$ is due to the presence of an ultrathin film of silicone oil (thickness: $d_{\mathrm{oil}} = 260$ nm, permittivity: $\varepsilon_{\mathrm{oil}} = 2$) which warrants lubrication of the solid surface [6, 7]. Finally, the surface tensions γ_{SG} and γ_{LG} being constant, the variation of γ_{SL}, expressed in term of the physicochemical surface pressure, Π_{SL}, writes, according to the latter equations:

$$\Pi_{SL} := \gamma_{SL_0} - \gamma_{SL}\,(0, C_0, t) = \gamma_{LG}\cos\theta\,(U, C_0, t) - \gamma_{LG_0}\cos\theta_0 - \frac{c}{8}U^2, \tag{2}$$

This last expression (2) illustrates how surface ageing must be corrected due to electrowetting.

4. DCA experiments with oscillating EWOD

Surface pressure measurements are carried out using imaging of the sessile drop in the course of time and extracting its contact angle (Figs. 1 – 2). The images are taken by switching off transiently the EWOD actuation during a short time scale (1s at most) no longer than the one required to damp drop oscillations under viscosity (about 100 ms, see Ref. [8]). Doing this, no impact on the averaged drop shape is observed except that the drop surface becomes clearly defined during this imaging step since the contact line stops to oscillate. Pure water and pure PBS buffer without electrowetting actuation were evaluated concerning their dynamic surface pressure. These model liquids are measured in order to check that the value of surface pressure remains at a constant level and therefore in order to validate our methodology (Fig. 2). The surface tension of 100%PBS buffer, γ_{LG_0} =75 mN/m, and the associated contact angle, $\theta_0 = 104°$, are chosen as reference values in eq. (1) or equivalently in eq. (2) with U=0.

In Fig. 2, pure water leads to a solid-liquid surface pressure apparently larger than the one of PBS buffer. This is in agreement with the fact that the PBS buffer is characterized by an averaged concentration of about

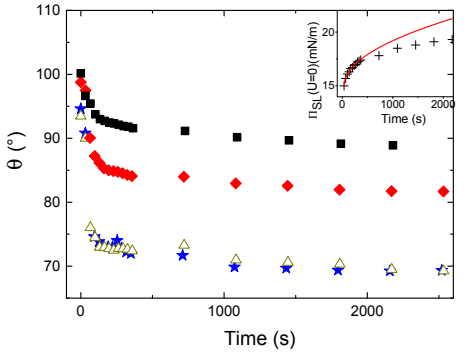

Fig. 1. Surface ageing as characterized by the reduction of the dynamic contact angle $\theta(t)$, for a 1 μ l-drop made from BSA (30 μg/mL) in 100% PBS buffer (pH = 4). Impact of oscillating electrowetting upon $\theta(t)$ for resonant eigenmodes (amplitude: $T_{n=2,4,6} = 0.15$): (♦) $n = 2$, (△) $n = 4$ and (★) $n = 6$. For sake of comparison, time dependence of the dynamic contact angle $\theta(t)$ (■) when electrowetting actuation is switched off. Insert: solid-liquid surface pressure $\Pi_{SL}(U = 0)$ (+) as deduced from eq. (1) and asymptotic fit (−) for the short-time diffusion-limited regime ($\Pi_{SL} \sim \sqrt{t}$ when $t \to 0$).

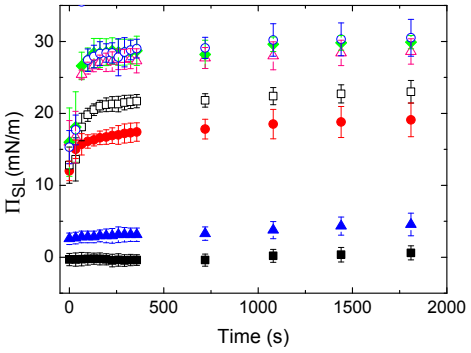

Fig. 2. Impact of oscillating electrowetting upon surface pressure Π_{SL} for a 1 µL-drop made from BSA 30 µg/mL in 100 % PBS buffer (pH = 4). Surface pressures are calculated from the reference surface tension γ_{LG_0}. Reference values (no EWOD actuation) of Π_{SL} as obtained from: ■ 100 % PBS buffer, ▲ pure water or ● BSA 30 µg/mL in 100 % PBS buffer. Dependence on both LF voltage amplitude and resonant modes: $n = 2$ (□ $T_2 = 0.15$, △ $T_2 = 0.30$), $n = 4$ (♦ $T_4 = 0.15$) and $n = 6$ (○ $T_6 = 0.15$).

150 mmol/L of different salts (typical of the physiological concentration of salts in biological cells) and has consequently a surface tension slightly larger than the one of pure water (see Eq. (1), keeping in mind that the contact angles of pure water as well as PBS buffer are both hydrophobic).

The experiments presented in this case focus on the aspect of low-frequency electrowetting and its impact on albumin adsorption on the lubricated solid substrate. Different resonant deformation modes, n = 2, 4 and 6, are investigated for different values of the normalized amplitude of drop deformation, $T_n = \dfrac{A_n}{R_0}$. The variables R_0 and A_n denote the drop radius and the amplitude of standing drop oscillations[7] for the eigenmode n. Contact angle measurements presented here are performed for $n = 2$ with T_2=0.15 or T_2=0.30 (Fig. 1). In addition, higher modes are compared ($n = 4$ and $n = 6$) for $T_n = 0.15$. For all measurements, electrowetting voltage U remains much smaller than the one required to initiate contact angle saturation (see e.g. Fig. 2 in Ref. [6]), so that the Lippmann-Young equation used in this paper always holds. The values of R_0 and A_n are extracted from imaging of drop oscillations. All relevant results are presented in Fig. 2 in term of surface pressure. Each data point is the mean value of a series of measurements performed in the same conditions and at the same time. In order to show the reproducibility, the standard deviation, σ, for each data point is calculated and displayed as an error bar.

PBS buffer with BSA and no EWOD actuation exhibits the least efficient surface ageing in the sense that the long time value of Π_{SL} ($t \to \infty$) still remains of the order of 19 mN/m. Then, by switching on EWOD actuation and by increasing the low frequency at constant drop oscillation amplitude, surface ageing is found to increase significantly. The higher mode, $n = 6$, reveals itself to be responsible for the most efficient surface ageing ($t \to \infty : \Pi_{SL} \sim 31$ mN/m). At first sight, this result could seem surprising since it is expected that the oscillatory shear generated by drop oscillations, prevents adhesion of the proteins to the substrate. This means that electrowetting-induced stirring due to steady streaming stands as an efficient means to enhance BSA transport towards the solid substrate. The impact of the amplitude of the modulation voltage at $n = 2$ is also investigated. Not surprisingly, the actuation amplitude also stands as a surface ageing enhancement parameter.

As also made evident in the experiments, the higher mode, $n = 6$ generates the most efficient surface ageing ($t \to \infty : \Pi_{SL} \sim 30$ mN/m, Fig. 2). And the numerical calculations of drop flow patterns [7] show that, in contrast to mode n=2 for which the vortices are observed throughout the drop, the vortices observed

at high mode, n=6, concentrate within the Stuart layer standing along the drop surface with a steady corner eddy located near the contact line [9]. This could explain why the efficiency of stirring-enhanced surface ageing might be higher for modes 4 and 6; a point which is in line with the presented measurements.

To support this physical interpretation, transient diffusive and convective transports of BSA molecules are calculated by taking into account drop streaming and adsorption at the solid substrate ([9]). The large value of the finiteness number, $\varepsilon_0 \sim 10$, means that the drop behaves as a semi-infinite system [10]. The large value of the Thiele number ($Th \sim 10 - 100$) indicates that solid-liquid surface ageing is essentially driven by a diffusion-limited regime without the presence of drop streaming flows. This is experimentally confirmed at short time without EWOD actuation (see insert in Fig. 1). The values of the Peclet and Damköhler numbers ($Pe \sim 10^6$, Da $\sim 10^{-4}$, see e.g.[9]) suggest that convection acts on shorter time scales than diffusion and adsorption, which confirms again that the influence of drop internal flows can not be neglected. Isoconcentration contours, as calculated from numerical simulations of BSA chemical transport, clearly demonstrate that a large concentration gradient arises near the contact line for high modes 4 and 6, while for mode 2, the most significant gradients are observed a little further to the center of the drop.

5. Conclusion

BSA molecules exhibit an affinity for the lubricated solid substrate underneath the drop, as demonstrated by a significant increase of the surface pressure Π_{SL}. The liquid-gas drop surface is also found to experience a significant change of its surface pressure Π_{LG} but due to the fast kinetics of drop surface ageing, it is not found dependent on EWOD actuation. The largest stirring efficiency is made evident near the contact line for a high resonant mode (n=6). The oscillating motion of the contact line under EWOD actuation can be interpreted as an efficient way to continuously adsorb and pack BSA molecules along the solid-liquid surface. Considering end-user needs, oscillating EWOD can deliver practical benefit to label free techniques [11] at digital scale, such as the one developed for a molecular recognition reaction in a solid-phase assay [4, 12]. By combining imaging of dynamic contact angle with oscillating EWOD at a large enough resonant mode (n = 6 for instance), in order to generate a steady eddy near the contact line, the detection sensitivity could be increased and the diagnostic speed up. Conversely, if the aim is to prevent biomolecular adsorption[13], EWOD at high frequency can be preferred to the oscillating regime.

References

[1] B. Berge, Electrocapillarity and wetting of insulator films by water, Vol. 317, Comptes Rendu de l'Academie des Sciences, 1993.
[2] C. Delattre, C. P. Allier, Y. Fouillet, D. Jary, F. Bottausci, D. Bouvier, G. Delapierre, M. Quinaud, A. Rival, L. Davoust, C. Peponnet, Macro to microfluidics system for biological environmental monitoring, Biosensors and Bioelectronics 36 (1) (2012) 230 – 235.
[3] M. G. Pollack, V. K. Pamula, V. Srinivasan, A. E. Eckhardt, Applications of electrowetting-based digital microfluidics in clinical diagnostics, Expert Review of Molecular Diagnostics 11 (2011) 393–407.
[4] P. Bergese, G. Oliviero, I. Colombo, L. Depero, Molecular recognition by contact angle: Proof of concept with DNA hybridization, Langmuir 25 (8) (2009) 4271–4273.
[5] T. T. Huang, J. Sturgis, R. Gomez, T. Geng, R. Bashir, A. K. Bhunia, J. P. Robinson, M. R. Ladisch, Composite surface for blocking bacterial adsorption on protein biochips, Biotechnology and Bioengineering 81 (5) (2003) 618–624.
[6] J. Theisen, L. Davoust, Dual-frequency electrowetting: Application to drop evaporation gauging within a digital microsystem, Langmuir 28 (1) (2012) 1041–1048.
[7] L. Davoust, Y. Fouillet, R. Malk, J. Theisen, Coplanar electrowetting-induced stirring as a tool to manipulate biological samples in lubricated digital microfluidics. impact of ambient phase on drop internal flow pattern, Biomicrofluidics 7 (4).
[8] J. Theisen, L. Davoust, Gauging contact line friction of droplets: in-situ measurement within a digital micro-system., Microelectron. Eng. 98 (2012) 680.
[9] J. Theisen, L. Davoust, Mass transfer enhancement and surface functionalization in digital microfluidics using ac electrowetting: the smaller, the better, Microfluidics and Nanofluidics 18 (5-6) (2015) 1373–1389.
[10] J. Theisen, L. Davoust, Surface ageing at drop scale, Microfluid. Nanofluid. 12 (1-4) (2012) 607.
[11] S. Ray, G. Mehta, S. Srivastava, Label-free detection techniques for protein microarrays: Prospects, merits and challenges, Proteomics 10 (4) (2010) 731–748.
[12] R. Bashir, R. Gomez, A. Sarikaya, M. R. Ladisch, J. Sturgis, J. P. Robinson, Adsorption of avidin on microfabricated surfaces for protein biochip applications, Biotechnology and Bioengineering 73 (4) (2001) 324–328.
[13] R. Garrell, J.-Y. Yoon, Preventing biomolecular adsorption in electrowetting-based biofluidic chips, Analytical Chemistry 75 (19) (2003) 5097–5102.